

# Preparation of Ni/biochar Catalyst for Hydrotreating of Bio-Oil from Microalgae Biomass

Hong K. D. Nguyen<sup>1</sup> · Vuong V. Pham<sup>2</sup> · Hai T. Do<sup>3</sup>

Received: 12 August 2016 / Accepted: 21 September 2016 / Published online: 1 October 2016  
© Springer Science+Business Media New York 2016

**Abstract** A new catalyst for hydrotreating process mainly including hydrodeoxygenation (HDO) and hydrodenitrogenation (HDN) was prepared by introducing Ni onto the surface of biochar obtained from microalgae biomass pyrolysis. The co-product bio-oil obtained from the pyrolysis was treated under H<sub>2</sub> pressure on the as-synthesized Ni/biochar catalyst. The whole process was established in a close loop cycle illustrating its high efficiency in comparison to other HDO or HDN processes. The catalyst was prepared through two-step procedure including biochar production and impregnating of Ni precursor onto the biochar. The pyrolysis of microalgal biomass was established at 400 °C for 2 h producing mainly the biochar and the bio-oil. The biochar was then doped with Ni<sup>2+</sup> by incipient wetness impregnation followed by drying and calcination at

suitable temperature for a certain time. The upgrading process including hydrodeoxygenation (HDO) and hydrodenitrogenation (HDN) reactions of bio-oil obtained from microalgal pyrolysis was investigated at various parameters such as temperature, time, catalyst dosage and stirring speed for converting bio-oil obtained from microalgal pyrolysis to rich hydrocarbon product. The Ni/biochar catalyst synthesized from the biochar through impregnation was used in the upgrading process. The results showed that the Ni/biochar catalyst could be very effective in the upgrading process producing mainly n-heptadecane as a very important component of diesel fuel. Some techniques were applied for characterizing the catalyst, feedstock and product such as XRD, H<sub>2</sub>-TPR, GC-MS and some standard ASTM methods.

---

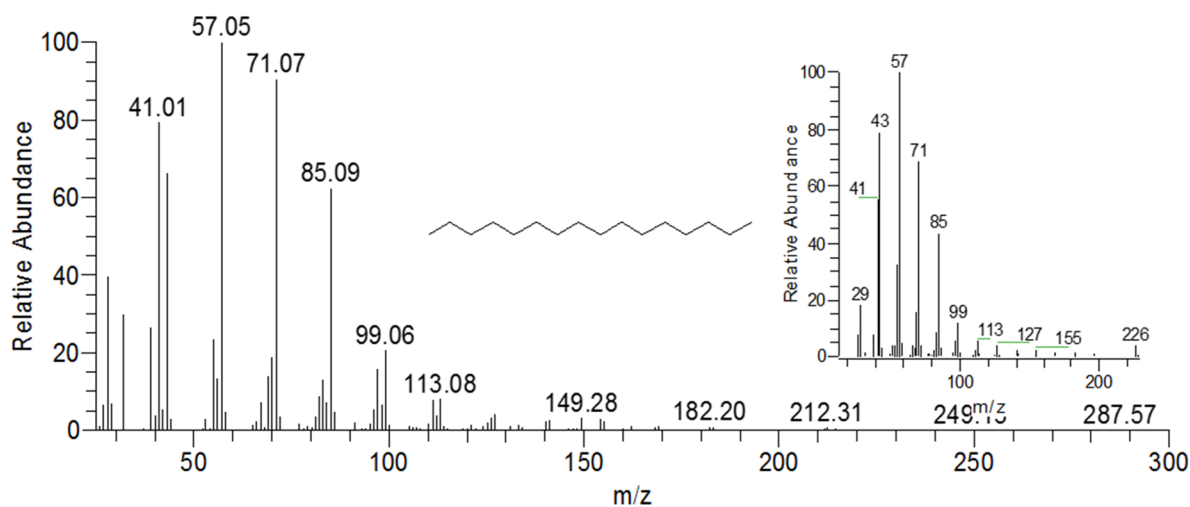
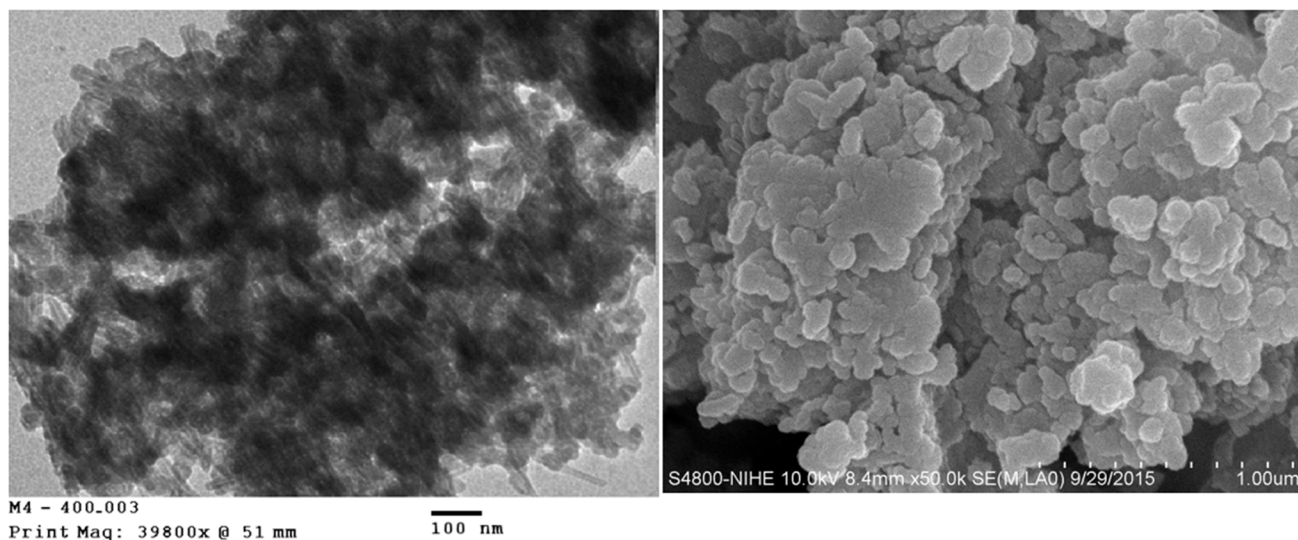
✉ Hong K. D. Nguyen  
dieuhongprof@gmail.com

<sup>1</sup> Hanoi University of Science and Technology, Hanoi, Vietnam

<sup>2</sup> Vietnam Oil and Gas Group, Hanoi, Vietnam

<sup>3</sup> Vietnam Institute of Industrial Chemistry, Hanoi, Vietnam

## Graphical Abstract



**Keywords** Biochar · Bio-oil · Upgrading · Microalgae · Ni/biochar

## 1 Introduction

Hydrotreating process was the removal of the heteroatom oxygen from the organic molecule in reaction with hydrogen forming water. The process was well known and took place in almost all HDS/HDN hydrotreaters today [1].

Generally the process used catalysts based on Co-MoS<sub>2</sub> and Ni-MoS<sub>2</sub> being similar to those used in the hydrotreating process of fossil feedstock; in which, Co or Ni served as promoters donating electrons to the molybdenum atoms. This weakened the bond between molybdenum and sulfur and thereby generated a sulfur vacancy site. These sites were the active centers in the HDN, HDS and HDO reactions [2].

Nowadays these catalysts have been also effectively used in the HDO and HDN process with bio-oil obtained from the pyrolysis of biomass. These trends promised producing many generations of cleaner, cheaper and more sustainable fuels such as green gasoline, green kerosene and green diesel [3].

The bio-oil produced from wood, vegetable oils and animal fats have been considered promising for delivering biofuels in large amount with low production cost. The abundance of oxygen and nitrogen in the form of various aliphatic and aromatic oxygenates and nitrogenates decreased the quality of bio-oil, however, and therefore the oxygen and nitrogen content must be reduced. Due to the low sulfur content of bio-oil, a sulphiding agent is typically added to the feed to maintain activity and stability of the catalysts. On the other hand, the hydrotreating processes in the fossil oil refinery were established with a small content of

heteroatoms (S, P, O, N...) in contrast of the large amount of oxygen or nitrogen in the bio-oil, so the traditional catalysts were quickly deactivated [1–3].

Recently we have found a new kind of catalyst which could be favorable applied in the hydrotreating process of the bio-oil feedstock. Our studies included some new contributions as followed: the catalyst could be applied at high temperature and pressure, large content of heteroatoms such as N, O...; there was no need for sulphiding of the catalyst like many other traditional process before introducing to the hydrotreating reactions; especially, the hydrotreating process over the catalyst could be performed nearly without by-products because the total process was established in a close loop cycle including pyrolysis of the microalgae biomass producing bio-oil and biochar, impregnation of suitable metal onto the biochar surface for metal/biochar catalyst and conversion of the obtained bio-oil to hydrocarbon using the metal/biochar catalyst. The close loop process could considerably enhanced performance of the HDO by reducing the price of the synthesized fuels and avoiding many environment effects.

This paper focused on preparation of the Ni/biochar catalyst followed by using it in the HDO process of the bio-oil with the mentioned new contributions.

## 2 Experimental

### 2.1 Preparation of the Ni/biochar Catalyst

The Ni/biochar catalysts were prepared by incipient wetness impregnation method. A series of Ni/biochar catalysts were prepared based on different concentration of the  $\text{Ni}(\text{NO}_3)_2$  solutions ranging from 0.2 to 3 M. The common procedure could be describes as follow.

Firstly a precise mass of biochar obtained from a slow pyrolysis process of microalgal biomass established at 400 °C for 2 h was measured for five catalyst samples. The biochar samples were uniformly grinded before transferring to the impregnation procedures.

Five solutions of  $\text{Ni}(\text{NO}_3)_2$  with concentrations of 0.2, 0.5, 1, 2 and 3 M were prepared by dissolving the salt in suitable volume of deionized water. Each solution was prepared in the volume of 20 ml. These solutions were used to well mixing with the five biochar samples under a vigorous stirring speed helping favorable diffusion of the  $\text{Ni}^{2+}$  onto the biochars.

The impregnations were performed at room temperature for 24 h followed by filtering the obtained solids until there was no appearance of  $\text{Ni}^{2+}$  cation (light blue color). The solids then were dried at 100 °C for 12 h and calcined at 400 °C for 4 h to obtain the Ni/biochar catalysts. The catalysts prepared at different concentration of the  $\text{Ni}(\text{NO}_3)_2$  solutions

were signed as NB-0.2, NB-0.5, NB-1, NB-2 and NB-3 exhibiting the corresponding concentrations of 0.2, 0.5, 1, 2 and 3 M respectively. These catalysts were characterized by XRD and  $\text{H}_2$ -TPR techniques. The catalyst was used for upgrading process in purpose of converting the bio-oil to rich hydrocarbon product.

### 2.2 Upgrading Process of Bio-Oil on the Ni/biochar Catalyst

The process was performed as follow:

- Firstly a certain mass of the Ni/biochar catalyst was activated by a reduction process to transfer  $\text{Ni}^{2+}$  to  $\text{Ni}^0$ . The reduction process was performed at 300 °C for 3 h in  $\text{H}_2/\text{N}_2$  flow (10% volume of  $\text{H}_2$ ) of 30 ml/min.
- Secondly the catalyst was transferred into a stirring supported batch reactor filled with a certain mass of the bio-oil. The  $\text{H}_2/\text{N}_2$  flow (10% volume of  $\text{H}_2$ ) was maintained during the process. The process was established at certain temperatures for precise times; stirring speed and catalyst dosage were also investigated after obtaining the suitable temperature and time.
- When the upgrading process was completed, the reactor was naturally cooled to room temperature followed by decantation of the liquid product from the solid catalyst. The liquid product was purified by distillation for separating the produced water, and the remained liquid was analyzed by GC-MS method to estimating the conversion of the bio-oil through the total remained oxygen content in the products in comparison to that of the feedstock.

### 2.3 Characterizations

Powder XRD of the samples were recorded on a D8 Advance Bruker diffractometer using  $\text{Cu K}\alpha$  ( $\lambda=0.15406$ )

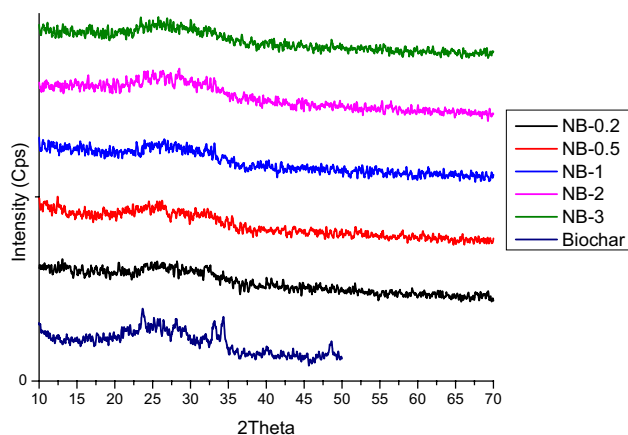


Fig. 1 XRD patterns of the Ni/biochar catalysts

radiation. SEM images were collected using Field Emission Scanning Electron Microscope S-4800. TEM images were recorded on a JEM1010-JEOL TEM operated at 80 kV. Nitrogen adsorption–desorption isotherm of the catalyst was recorded on a Micromeritics Gemini VII 2390 V1.02 at 77 K with pre-degasification at 423 K for 2 h under high vacuum. H<sub>2</sub>-TPR measurements were established on AutoChem II 2920 Micromeritics and Micromeritics AutoChem II 2920 V4.01. FT-IR spectroscopies were measured on Nicolet 6700 FT-IR Spectrometer. GC-MS was established on an Agilent HP 6890 GC-5898 MS supported capillary HT-5MS.

### 3 Results and Discussions

#### 3.1 XRD Patterns of the Ni/biochar Catalysts

Figure 1 described the XRD patterns of the catalysts NB-0.2, NB-0.5, NB-1, NB-2, NB-3 and biochar.

The XRD patterns of the samples showed domination of amorphous structure from the biochar to the Ni/biochar catalysts. There was a small different in the patterns of the biochar in comparison to the others which could be assumed for some structure changes from the biochar to the Ni/biochar catalysts such as the incorporating the Ni<sup>2+</sup> cations into the surface or even in bonding network of the biochar. For the catalysts there were very similar patterns among them whatever they were prepared from the different concentration of Ni<sup>2+</sup> exhibiting the same amorphous structures of the five catalysts. There were also no trace of crystalline of NiO, Ni(OH)<sub>2</sub> or any kind of Ni based compounds detected in all the catalysts demonstrating the very uniform distribution of the NiO particles on the catalyst surface. This uniform

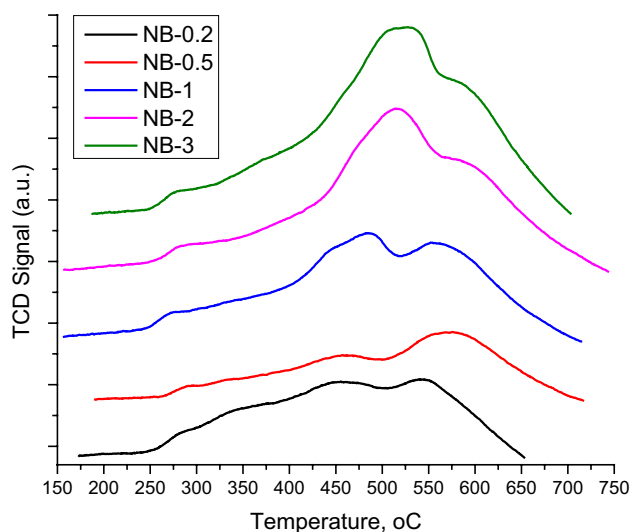


**Fig. 2** H<sub>2</sub>-TPR diagrams of the Ni/biochar catalysts

**Table 1** H<sub>2</sub>-TPR results of the Ni/biochar catalysts

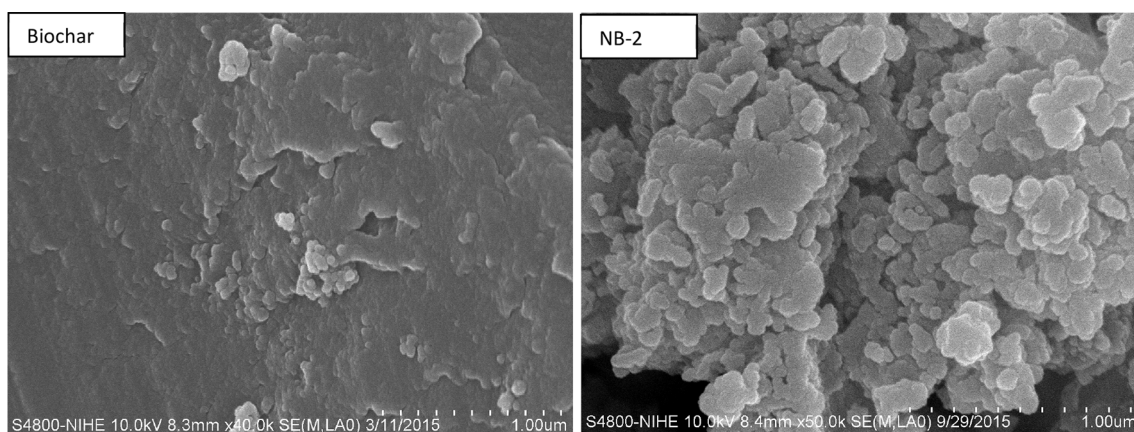
No.	Reduction peak (°C)	H <sub>2</sub> consumption (mmol/g)
NB-0.2	215.8	0.01671
	291.1	0.11223
	347.8	0.35726
	453.1	0.84561
	536.9	0.53956
	585.3	0.47931
NB-0.5	286.9	0.01288
	337.0	0.15554
	462.3	0.47594
	537.9	0.28122
	590.1	0.36905
	642.6	0.22563
NB-1	273.0	0.05907
	337.8	0.31390
	459.7	1.19883
	508.5	0.38191
	569.6	1.05544
	644.3	0.26038
NB-2	288.4	0.06943
	444.2	1.28235
	483.5	0.45003
	522.4	0.68493
	592.5	0.97467
	661.3	0.40975
NB-3	287.1	0.12595
	373.7	0.28979
	485.0	0.77307
	530.7	0.33094
	566.5	2.22956
	658.8	0.22706

distribution was also an advantage for the activity of the catalyst in the mentioned HDO process.

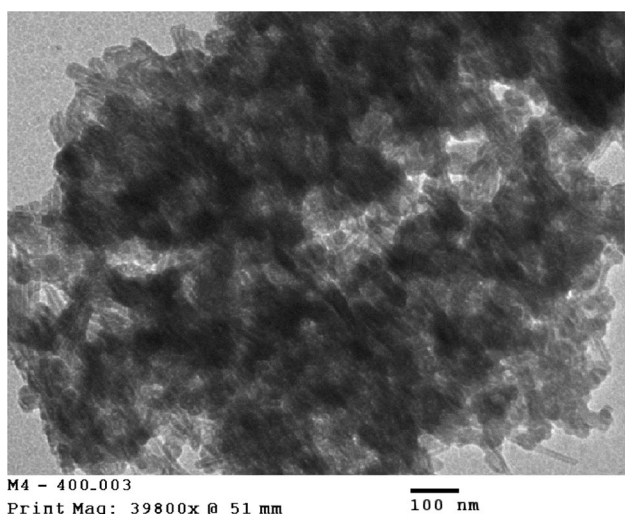
#### 3.2 H<sub>2</sub>-TPR Results of the Ni/biochar Catalysts

Figure 2 described the H<sub>2</sub>-TPR results of the NB-0.2, NB-0.5, NB-1, NB-2 and NB-3 catalysts, and the peak temperature of reduction and the TCD concentrations were also collected (Table 1).

Generally the peak temperature of reductions of the Ni/biochar catalysts reflected the stability of the Ni<sup>2+</sup> portions on the catalyst surface as the reduction temperature was lower than 400 °C or higher than 500 °C corresponding to the reduction of the bulk NiO portions, the Ni-support weak interactions or the Ni-support strong interactions respectively [4]. There were a common tradition observed when comparing different TPR results obtained from the different catalysts that peak temperature of the reductions



**Fig. 3** SEM images of the biochar and the Ni/biochar catalyst



**Fig. 4** TEM image of the NB-2 catalyst

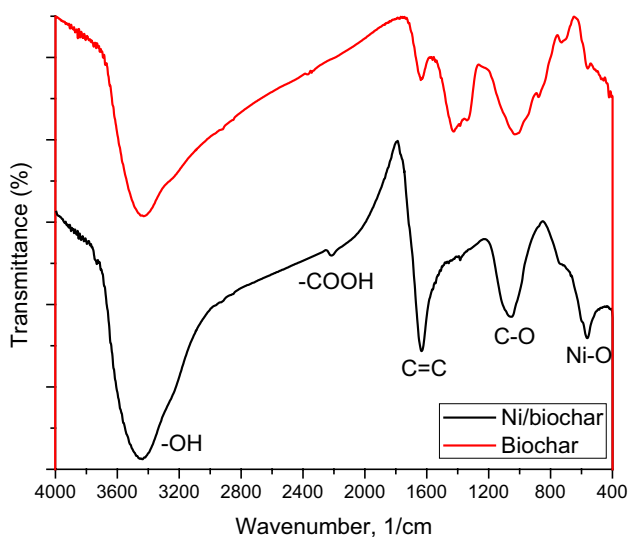


**Fig. 5** FT-IR spectroscopies of the biochar and NB-2 catalyst

gradually increased from the NB-0.2 to NB-2 catalysts and slightly decreased with the NB-3 catalyst. These results could be caused by the higher concentration of the  $\text{Ni}^{2+}$  in the impregnation solution strengthening the loading capacity and the diffusion of  $\text{Ni}^{2+}$  onto the catalyst surface. The consequence was to enhance the Ni-support interactions beside the bulk NiO. However when the concentration of the impregnation solution was too high as in the preparation of the NB-3 catalyst, the NiO portions could cover the biochar surface with multilayers leading to agglomerate in the calcination and the reduction processes. This phenomenon weakened the Ni-support interactions revealing the decrease of the reduction peak temperature. The NB-2 catalyst showed a favorable density of the Ni-support strong interactions with considerable  $\text{H}_2$  consumption that was important in the HDO process because its stability and good activity. Therefore we used the NB-2 catalyst in the HDO process for upgrading the bio-oil obtained from the pyrolysis of the microalgal biomass.

Particularly, the results obtained from the analysis of the NB-2 catalyst showed six reduction peaks corresponding to six states of the connections between the NiO and the biochar at different temperatures. In which, the peak at  $288.4^\circ\text{C}$  could be assigned to the reduction of the bulk NiO portions weakly attaching to the support; the peak at  $444.2$ ,  $483.5$  and  $522.4^\circ\text{C}$  corresponded to the NiO portions connected with the biochar at medium strength through  $\text{Ni-O-C}_{\text{support}}$  (referred to the FT-IR spectroscopy analysis in 3.4); the peak at  $592.5$  and  $661.3^\circ\text{C}$  characterized for the NiO portions with strong bonds with the support. As mentioned, the connections with medium strength between the NiO with biochar were the most suitable for the catalysts activity. Assuming that all the NiO portions were reduced from  $\text{Ni}^{2+}$  to  $\text{Ni}^0$ , then the generated Ni site density was equal to the moles of the consumed hydrogen during the reduction. Therefore, the amount of the suitable connected

**Fig. 6** Adsorption–desorption isotherms of the NB-2 catalyst

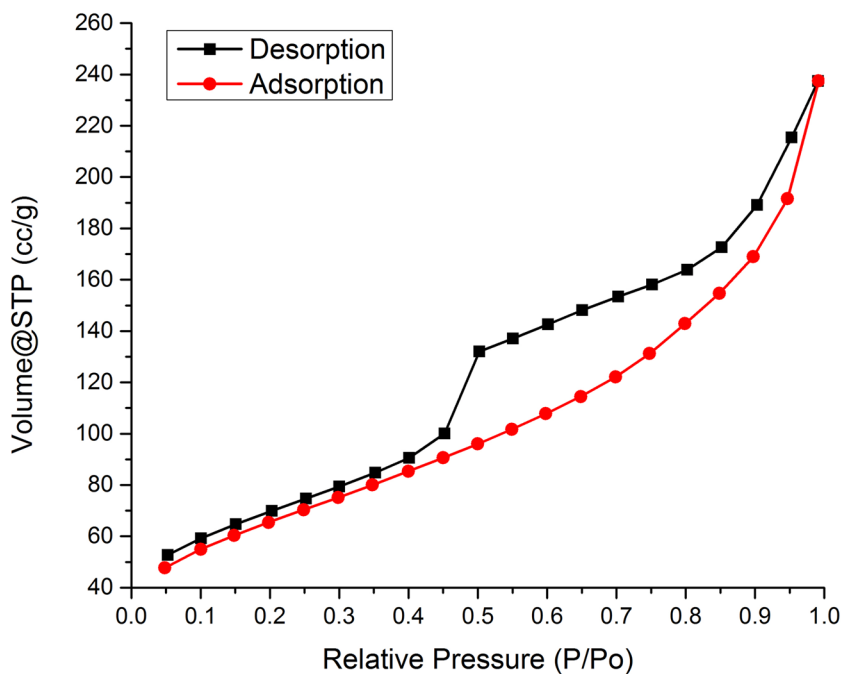
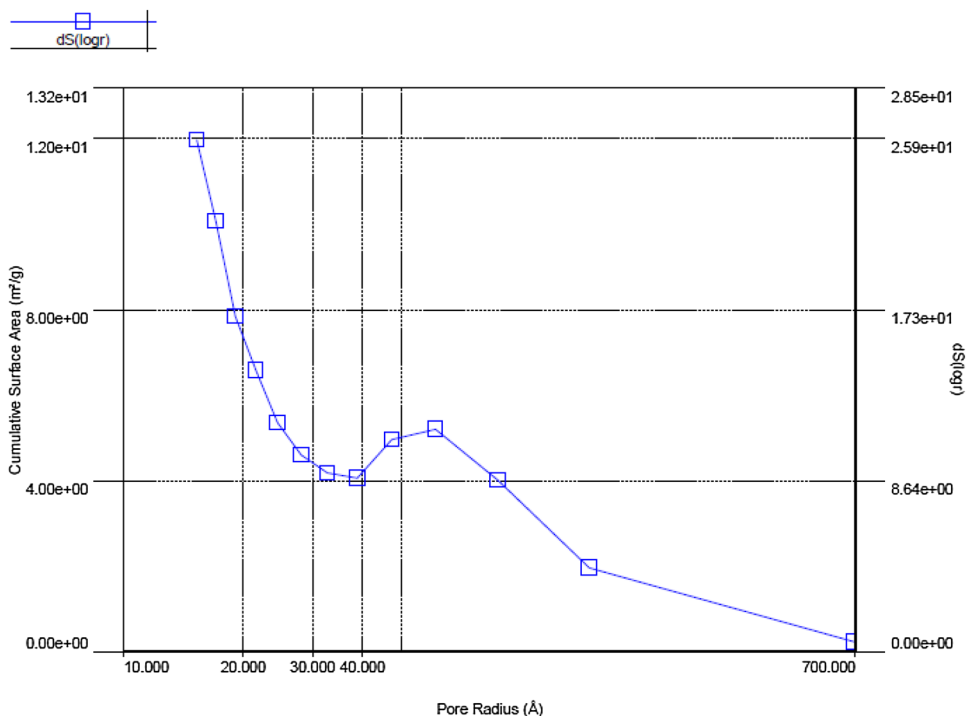


**Fig. 7** Pores distribution of the NB-2 catalyst



NiO portions with medium strength took an account for  $(1.28235 + 0.45003 + 0.68493)/(0.06943 + 1.28235 + 0.45003 + 0.68493 + 0.97467 + 0.40975) = 62.44\%$  of the total amount of the NiO located on the biochar surface. The high percentage of the active NiO portions on the biochars surface considerably enhanced the catalysts activity in the oxidation–reduction processes.

### 3.3 SEM Images of Biochar and NB-2 Catalyst

Figure 3 showed the SEM images of the biochar and the NB-2 catalyst. In the same implications, the SEM images clearly indicated difference in morphology of the two materials: the biochar mainly contained uniform 20 nm sized particles agglomerated together producing a large clusters

**Table 2** Specifications of the bio-oil

STT	Specifications	Methods	Values
1	Density at 15.5 °C	D 1298	0.96
2	Flash point (°C)	D 92	31
3	Viscosity (40 °C, mm <sup>2</sup> /s)	D 445	0.8
4	Pouring point (°C)	D 127	−35.2
5	Distillation	D 86	
	Initial boiling point (°C)		160
	10% (°C)		185
	50% (°C)		265
	90% (°C)		330
	Final boiling point (°C)		335
6	Acid value (mgKOH/g)	D 664	0.53
7	Heating value (MJ/kg)	D 240	29.6
8	Water content (mg/kg)	D 95	18
9	Color	–	Dark, transparent
10	Odor	–	Special

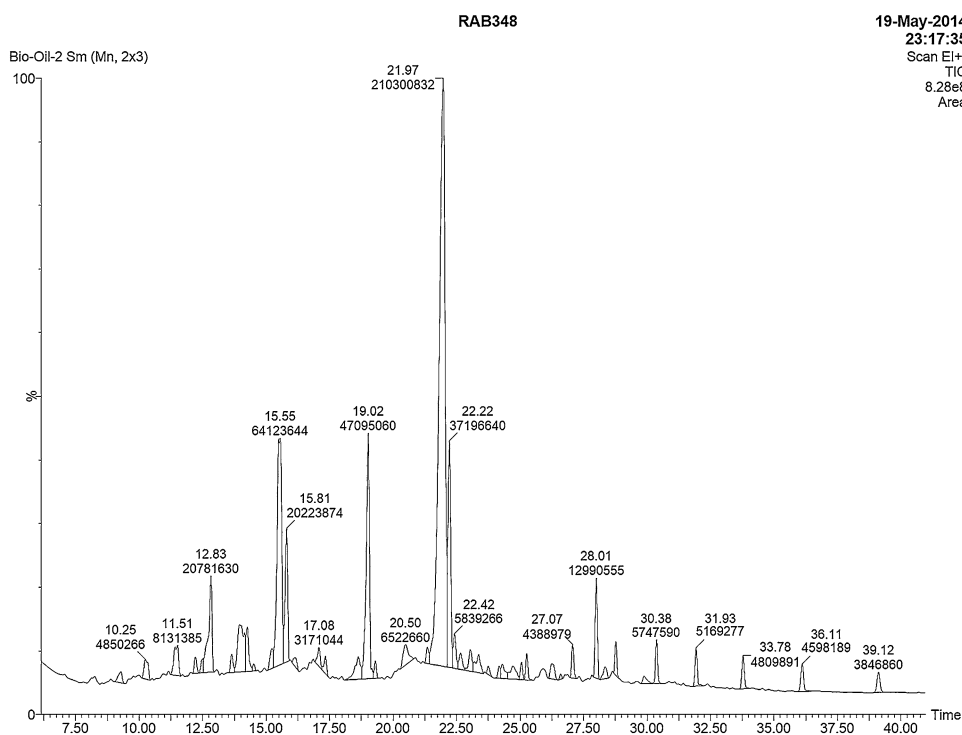
while the catalyst consisted of small thin size particles arranged in the layer structure beside the same clusters as the biochars morphology. The observations were suitable to the different results obtained from the XRD patterns confirming that the NiO and Ni portions on the catalyst surface existed in the amorphous states. The Ni distribution was well looked in the TEM images.

### 3.4 TEM Images of the NB-2 Catalyst

Figure 4 showed the TEM image of the NB-2 catalyst. There was many dark regions distributed along with light background corresponded to the Ni clusters on the bio-char surface respectively. The dark regions with size about 30–50 nm could be assigned for the agglomeration of the Ni metals during the calcination and the reduction of the catalyst. An interesting observation was obtained when occurring some long bar morphologies indicating the formation of carbon nanotubes [5, 6]. This structure could be generated during the pyrolysis of the microalgal biomass. The carbon nanotubes possessed mesoporous structure, so they could be useful for increasing diffusion ability of the Ni clusters on the catalysts surface and avoiding the overagglomeration of the active sites during the calcination.

### 3.5 FT-IR Spectra of Biochar and NB-2 Catalyst

Figure 5 revealed the FT-IR spectroscopy of the biochar and NB-2 catalyst. The analysis results pointed out appearances of many the same organic functions in the polycyclic aromatic system of the biochar and catalyst including –OH phenolic groups at ~3400 cm<sup>-1</sup>, –OH carboxylic acid at ~2200 cm<sup>-1</sup> and C=C aromatic rings at ~1650 cm<sup>-1</sup>. These results reflected the same framework of the biochar and the catalyst. Especially with the NB-2 catalyst, there were

**Fig. 8** GC diagram of the bio-oil

**Table 3** Chemical composition of the bio-oil

No.	Name	Formula	Contents, %
1	6-Methyl-octadecane	C <sub>19</sub> H <sub>40</sub>	0.55
2	4-Trifluoroacetoxytridecane	C <sub>15</sub> H <sub>27</sub> F <sub>3</sub> O <sub>2</sub>	1.04
3	2,6,10-Trimethyl-tetradecane	C <sub>17</sub> H <sub>36</sub>	1.75
4	Hexadecane	C <sub>16</sub> H <sub>34</sub>	4.46
5	9-Hexadecenoic acid	C <sub>16</sub> H <sub>30</sub> O <sub>2</sub>	4.02
6	2-Methyl-E-7-hexadecene	C <sub>17</sub> H <sub>34</sub>	13.77
7	Heptadecane	C <sub>17</sub> H <sub>36</sub>	4.34
8	9-Hexadecenoic acid	C <sub>16</sub> H <sub>30</sub> O <sub>2</sub>	0.68
9	Oleic Acid	C <sub>18</sub> H <sub>34</sub> O <sub>2</sub>	2.08
10	Hexadecanenitrile	C <sub>16</sub> H <sub>31</sub> N	10.11
11	Oleanitrile	C <sub>18</sub> H <sub>33</sub> N	45.16
12	Octadecanenitrile	C <sub>18</sub> H <sub>35</sub> N	7.99
13	3-Pentyl-, methyl ester, trans-oxiraneundecanoic acid	C <sub>19</sub> H <sub>36</sub> O <sub>3</sub>	1.25
14	Diisooctyl-1,2-benzenedicarboxylate	C <sub>24</sub> H <sub>38</sub> O <sub>4</sub>	2.79

**Table 4** Results obtained from the investigations of the upgrading process

Temperature (°C)					
Value	150	200	250	300	350
Yield (%)	20.2	35.2	50.2	64.2	64
Time (h)					
Value	0.5	1	1.5	2	2.5
Yield (%)	31.5	49.8	60.1	68.5	68.5
Catalyst content (%)					
Value	2	3	4	5	6
Yield (%)	35.9	52.3	61.7	70.1	70.1
Stirring speed (rpm)					
Value	100	200	300	400	500
Yield (%)	49.2	54.9	65.3	71.1	71.2

additions of Ni–O vibration at  $\sim 510\text{ cm}^{-1}$  assigning for a redshift from that of the bulk NiO at  $\sim 460\text{ cm}^{-1}$  [7] demonstrating the appearance of Ni–O–C bonds formed by NiO and the support through oxygen bridges. The partial transference of electron density from Ni–O to the polycyclic aromatic system could be corresponded for this phenomenon. There was also an absence of Ni–C connections illustrating none of the carbon bridges occurring like Ni–C<sub>support</sub> connections. In addition, the redshift could not be observed when considering the Ni–C<sub>support</sub> because the Ni<sup>2+</sup> portions always pulled the electron from the aromatic system through the conjugation effect reducing the electron density of this system.

### 3.6 BET Measurement of the NB-2 Catalyst

The adsorption–desorption isotherm of the NB-2 catalyst described in Figs. 6 and 7 indicated a large hysteresis between the adsorption and desorption curves including the characterization of the appeared mesoporous structure. The BET surface area reached  $65.712\text{ m}^2/\text{g}$  proved that the amount of the mesopores were not as high as some typical mesoporous materials such as MCM-41 or SBA-15. The pore distribution also confirmed these conclusions when showing a range of pore diameters focusing at  $40\text{ \AA}$ . The mesopores could be assigned for the generation of the carbon nanotubes observed in the TEM image of the catalyst. Otherwise, the pore distribution haven't concentrated on the narrow diameters demonstrating the amount of the carbon nanotubes was low.

### 3.7 Establishing the Upgrading Process on the NB-2 Catalyst

Firstly, the specifications of the bio-oil were determined using standard methods, and Table 2 described these values.

The specifications of the bio-oil contained many values which was not satisfied for many applications including motor fuels such as low heating value, high water content. The reason could be assigned for its high content of heteroatoms such as oxygen and nitrogen. Secondly, the bio-oil was analyzed to determine its chemical composition before entering the upgrading process. Figure 8 described the GC diagram of the bio-oil.

Table 3 showed the bio-oil chemical composition. The results showed that there were a large amount of oxygenates and nitrogenates which need to be removed through the hydrotreating establishment. There was a distinguishable property of the bio-oil obtained from microalgal biomass than the other biomass: the nitrogen content in the oil was very high in comparison to the oxygen content because the high content of nitrogen element in the original biomass [1, 2]. The investigations of this process was detail described in the Table 4.

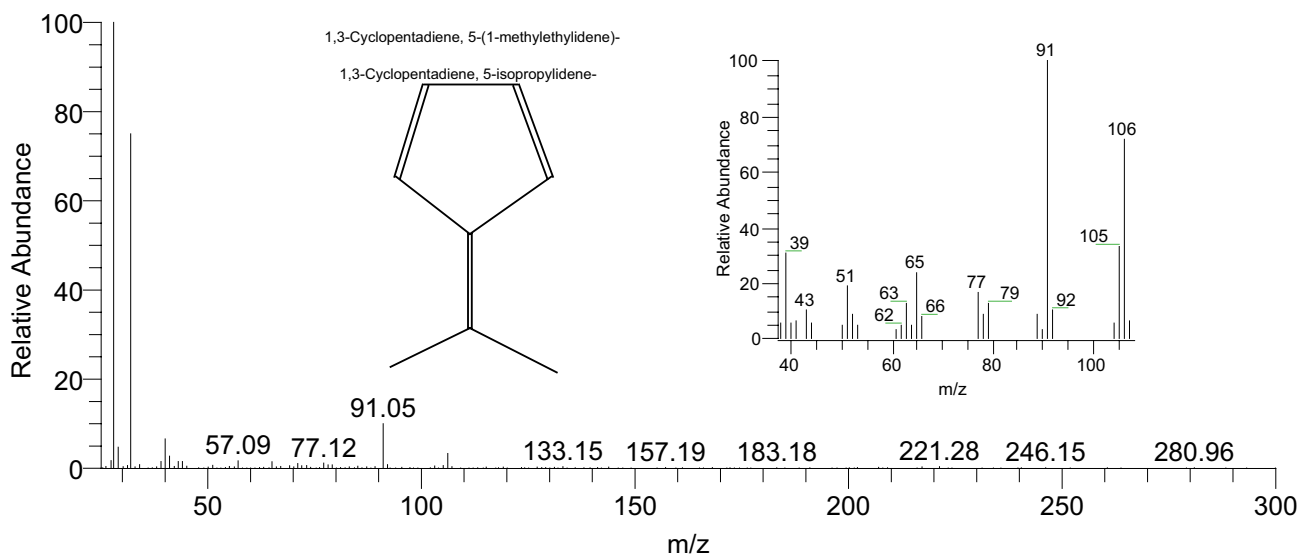
The results revealed a collection of optimum parameters such as temperature of  $300\text{ }^\circ\text{C}$ , time of 2 h, catalyst content of 5%wt and stirring speed of 400 rpm. The maximum yield of the process reached 71.1% demonstrating the very high activity and selectivity of the NB-2 catalyst. After the upgrading process, the liquid product was also analyzed by GC-MS method to find its chemical composition. Figure 9 and Table 5 described these results.

There were also some typical MS demonstrations representing for 5-(1-methylethylidene)-cyclopentadiene and hexadecane in chemical composition of the upgrading product.



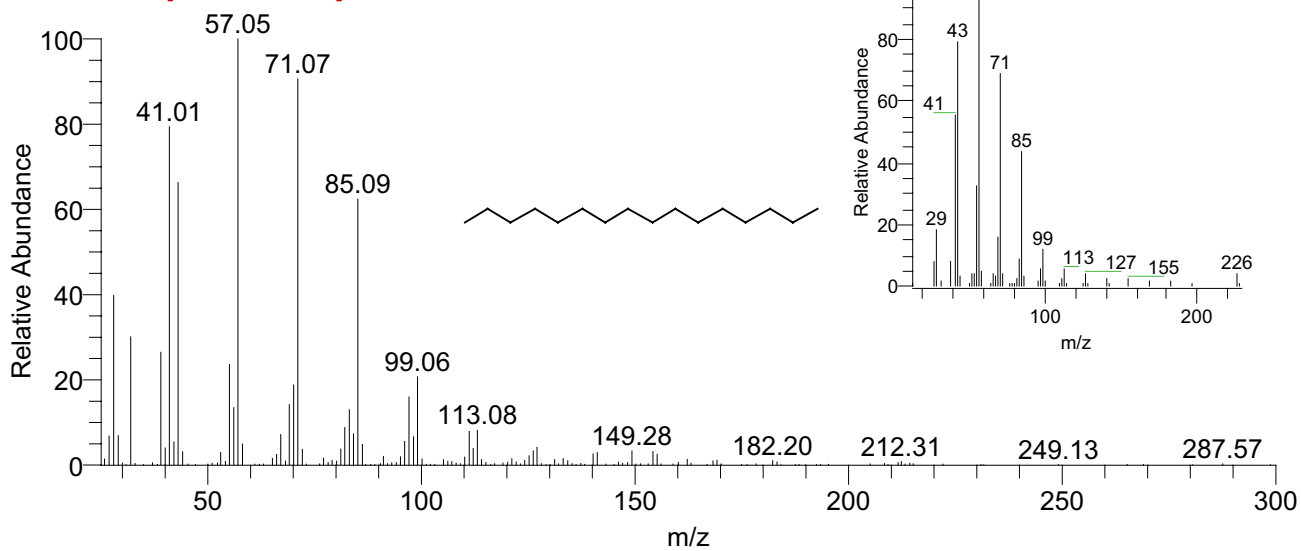
toan\_1-6-2016 #113 RT: 4.64 AV: 1 NL: 2.47E5

F: + c Full ms [ 25.00-300.00]

**5-(1-methylethylidene)-cyclopentadiene**

toan\_1-6-2016 #1381 RT: 11.87 AV: 1 NL: 2.31E5

F: + c Full ms [ 25.00-300.00]

**Hexadecan**

**Fig. 9** GC diagram of the liquid product obtained from the upgrading process

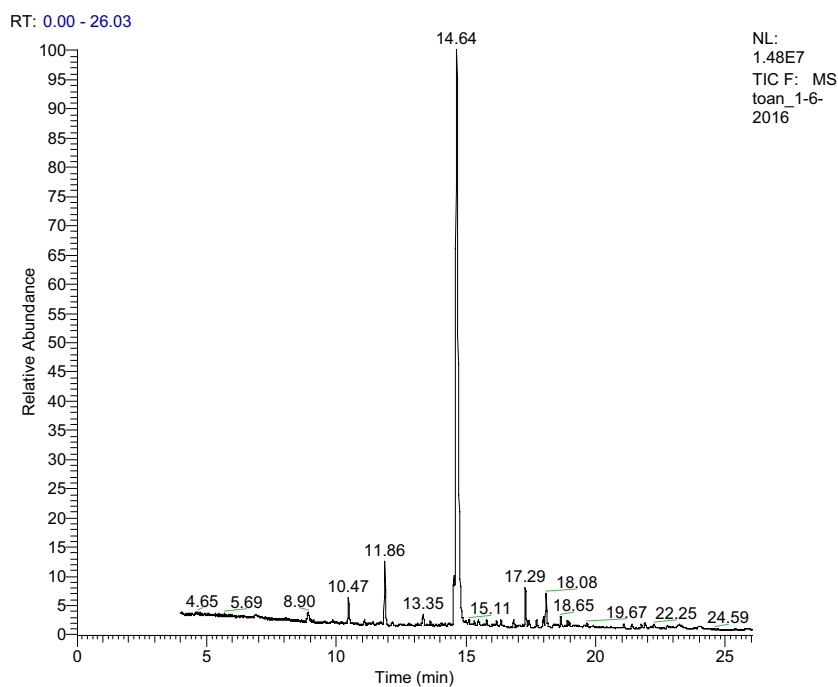


**Table 5** Chemical composition of the liquid product obtained from the upgrading process

No.	Names	Formulas	Contents (%)
1	5-(1-Methylethylidene)-cyclopentadiene	C <sub>8</sub> H <sub>10</sub>	0.41
2	2,6,7-Trimethyl-decane	C <sub>13</sub> H <sub>28</sub>	0.44
3	2,6,10-Trimethyl-dodecane	C <sub>15</sub> H <sub>32</sub>	1.19
4	6-Propyl-tridecane	C <sub>16</sub> H <sub>34</sub>	1.79
5	2,6,10-Trimethyl-tetradecane	C <sub>17</sub> H <sub>36</sub>	0.39
6	Methyl-10,13-octadecadiynoate	C <sub>19</sub> H <sub>30</sub> O <sub>2</sub>	0.32
7	Cis-(−)-2,4a,5,6,9a-hexahydro-3,5,5,9-tetramethyl(1H) benzocycloheptene	C <sub>15</sub> H <sub>24</sub>	0.41
8	Hexadecane	C <sub>16</sub> H <sub>34</sub>	4.00
9	10-12-Pentacosadiynoic acid	C <sub>25</sub> H <sub>42</sub> O <sub>2</sub>	0.34
10	Methyl octadecadiynoate	C <sub>19</sub> H <sub>30</sub> O <sub>2</sub>	0.33
11	7-Ethynyl-naphthalenone	C <sub>14</sub> H <sub>18</sub> O	0.31
12	2,6,10-Trimethyl-tetradecane	C <sub>17</sub> H <sub>36</sub>	1.09
13	Bi-1-cycloocten-1-yl	C <sub>16</sub> H <sub>26</sub>	0.48
14	n-Heptadecane	C <sub>17</sub> H <sub>36</sub>	75.68
15	3,4-Dihydro-4,7,8-trimethyl-naphthalenone	C <sub>13</sub> H <sub>16</sub> O	0.38
16	2-Butyl-naphthalene	C <sub>14</sub> H <sub>16</sub>	0.52
17	Benzocycloheptatriene	C <sub>11</sub> H <sub>10</sub>	0.66
18	2,4-Dimethyl-phenol	C <sub>8</sub> H <sub>10</sub> O	0.51
19	2-Ethyl-6-methyl-phenol	C <sub>9</sub> H <sub>12</sub> O	0.38
20	Cyclonon-4-ynone	C <sub>9</sub> H <sub>12</sub> O	2.69
21	2,7-Dimethyl-naphthalene	C <sub>12</sub> H <sub>12</sub>	0.60
22	2,5-Diethylphenol	C <sub>10</sub> H <sub>14</sub> O	0.61
23	2,4-Dimethyl-phenol	C <sub>8</sub> H <sub>10</sub> O	3.07
24	Methyl-6,9,12,15-docosatetraenoate	C <sub>23</sub> H <sub>38</sub> O <sub>2</sub>	0.32
25	Methyl oxiraneoctanoate	C <sub>19</sub> H <sub>36</sub> O <sub>3</sub>	0.41
26	3,4,4-Trimethyl-3-[(1E)-3-methyl-1,3-butadienyl]bicyclo[4.1.0]heptan-2-one	C <sub>15</sub> H <sub>22</sub> O	0.65

**Table 5** (continued)

No.	Names	Formulas	Contents (%)
27	4-(2,6,6-Trimethyl-2-cyclohexen-1-yl)-3-buten-2-one	C <sub>13</sub> H <sub>20</sub> O	0.6
28	1,8,15,22-Tricosatetrayne	C <sub>23</sub> H <sub>32</sub>	0.41
29	13-Heptadecyn-1-ol	C <sub>17</sub> H <sub>32</sub> O	0.52
30	2-Methyl-5-[3-indolylmethyl]-4,5-dihydroimidazole-4-one	C <sub>13</sub> H <sub>13</sub> N <sub>3</sub> O	0.49

The hydrocarbon content in the upgraded product reached up to over 80% demonstrating the favorable performance of the reaction. The very high content of n-heptadecane took an advantage of using this kind of product in the diesel fraction. However, there were some tiny amount of many oxygenates and nitrogenates which had to be separated from this product. Therefore it required a purification procedure such as distillation for reduce these heteroatom containing molecules. The Ni/biochar catalyst NB-2 accelerated both HDO and HDN processes, especially reducing the nitrogenates from 63.26 to 0.49%, so this was one of the advanced catalyst for the bio-oil upgrading.

#### 4 Conclusion

The Ni/biochar catalyst possessed amorphous phases generated through combination of biochar, NiO and Ni clusters. The catalyst also contained a dominative amount of medium-strength interactions between the NiO clusters and the biochar through Ni–O–C connections. The texture and morphology properties of the catalyst showed the existence of mesoporous structure and a small suppressed amount of coexisted carbon nanotubes. The suitable connected NiO portions on the biochar surface were high could play an important role in strengthening the activity of the catalyst in the HDO process. The catalyst possessed amorphous structure, high content of medium Ni-support connections improving the stability of the Ni species on the catalyst surface. This properties also provide good potential of application in the upgrading process of the bio-oil.

The upgrading process produced liquid product containing a large amount of hydrocarbon, especially

n-heptadecane, which was very convenient for blending with diesel fraction. Both oxygenates and nitrogenates were sharply reduced through HDO and HDN processes demonstrating the high activity and selectivity of the Ni/biochar catalyst. However, because of small amount of oxygenates and nitrogenates, the further purification was required for enriching the hydrocarbon content of the product.

#### References

1. Donniss B, Egeberg RG, Blom P, Knudsen KG (2009) Hydroprocessing of bio-oils and oxygenates to hydrocarbons. Understanding the reaction routes. *Top Catal* 52:229–240
2. Mortensen PM, Grunwaldt J-D, Jensen PA, Knudsen KG, Jensen AD (2011) A review of catalytic upgrading of bio-oil to engine fuels. *Appl Catal A Gen* 407:1–19
3. Carlson TR, Tompsett GA, Conner WC, Huber GW (2009) Aromatic production from catalytic fast pyrolysis of biomass-derived feedstocks. *Top Catal* 52:241–252
4. Yingxin L, Jixiang C, Jiyan Z (2007) Effects of the supports on activity of supported nickel catalysts for hydrogenation of m-dinitrobenzene to m-phenylenediamine. *Chin J Chem Eng* 15(1):63–67
5. Lia XF, Luo XG (2014) Preparation of mesoporous activated carbon supported Ni catalyst for deoxygenation of stearic acid into hydrocarbons. *Environ Prog Sustain Energy* 0:1–6
6. Özkan G, Gök S, Özkan G (2011) Active carbon-supported Ni, Ni/Cu and Ni/Cu/Pd catalyzed steam reforming of ethanol for the production of hydrogen. *Chem Eng J* 171:1270–1275
7. Barakat A, Al-Noaimi M, Suleiman M, Aldwayyan AS, Hammouti B, Hadda TB, Haddad SF, Boshala A, Warad I (2013) One step synthesis of NiO nanoparticles via solid-state thermal decomposition at low-temperature of novel aqua(2,9-dimethyl-1,10-phenanthroline)NiCl<sub>2</sub> complex. *Int J Mol Sci* 14:23941–23954